Performance of the AMS-02 Electromagnetic Calorimeter in Space

STEFANO DI FALCO[1] FOR THE AMS-02 ECAL GROUP.

[1] *INFN Pisa, Italy.*

stefano.difalco@pi.infn.it

Abstract: The Alpha Magnetic Spectrometer (AMS-02) is an high-energy particle detector deployed on the International Space Station (ISS) since May 19, 2011 to conduct a long-duration mission on fundamental physics research in space. The main scientific goals of the mission are the detection of antimatter and dark matter through the study of the spectra and fluxes of protons, electrons, nuclei until the iron, their antiparticles, and gamma-rays in the GeV to TeV energy range. The Electromagnetic CALorimeter (ECAL) is required to measure e^+, e^- and gamma spectra and to discriminate electromagnetic showers from hadronic cascades. To fulfill these requirements the ECAL is based on a lead/scintillating fiber sandwich, providing a 3 Dimensional imaging reconstruction of the showers. The high granularity consists of 18 samplings in the longitudinal direction, and 72 samplings in the lateral direction. Measurements of ECAL parameters in space and performance in term of energy and angular resolutions, linearity, proton rejections will be reviewed.

Keywords: icrc2013, calorimeter, AMS.

1 Introduction

The Alpha Magnetic Spectrometer (AMS-02) is an high-energy particle detector that is successfully operating on board of the International Space Station (ISS). Its main components, described in detail in [1], are:

- a permanent magnet and a Silicon Tracker, to measure the particle momentum and charge;
- a Time of Flight (TOF) system, to measure the particle velocity and charge and to give the trigger for the charged particles;
- a Transition Radiation Detector (TRD), to separate hadrons from electrons, to measure partcile charge and to perform a rough tracking of charged particles;
- a Ring Imaging Cherenkov counter (RICH), to measure velocity and charge of particles and nuclei;
- an Electromagnetic Calorimeter (ECAL), to measure the energy of electromagnetic particles and reconstruct their direction and to furnish a trigger for them, including photons.

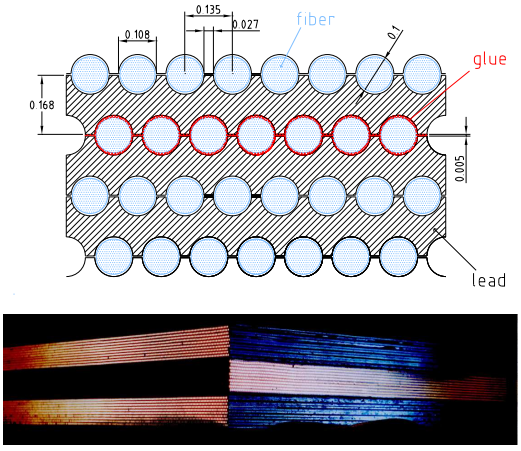

Figure 1: ECAL active part structure: lead and fiber layers are alternated; each 10 fiber layers (*superlayer*) the fiber orientation is rotated by 90 degrees.

2 The AMS-02 Electromagnetic Calorimeter

The active part of the AMS-02 Electromagnetic Calorimeter (ECAL)[2] is a fine grained pancake of lead and scintillating fibers (Fig.1.a).

The main parameters of the pancake are reported in table 1.

Fiber orientation is rotated by 90 degrees each 10 layers of lead and fibers. Each 10 lead and fiber layers define a *superlayer* (Fig.1.b). Perpendicularly to the detector axis, there are 5 superlayers with fiber aligned along the magnetic bending direction (Y) and 4 superlayers with fibers aligned along the other direction (X).

Light from the fibers is collected by light guides and sent to 4-anode Hamamatsu R7600-00-M4 photomultipliers (PMTs), arranged alternatively on the two opposite ends of the fibers in order to minimize the dead areas.

Each anode signal is sent to the Front End Electronics and split in two: one copy of the signal is digitized as it is ("low gain ADC"), the other is amplified by a factor 33 ("high gain ADC"). The double ADC scale allows for a larger dynamical range while maintaining the wanted resolution on the very low signals deposited by the minimum ionizing particles (MIPs).

The last dynode of each PMT of the 6 central superlayers is also split in two: a copy is sent to an ADC and written in the data stream, the other is discriminated to form a trigger bit used in the ECAL trigger for electromagnetic particles [3].

Dimensions	$64.8 \times 64.8 \times 16.65\, cm^3$
Materials volume	Lead/Fibers/Glue (58/33/9 %)
Weight	488 Kg
Density	$6.83\, g/cm^3$
Radiation lenght	$X_0 \sim 1$ cm
Superlayers	5(Y view), 4(X view)

Table 1: AMS-02 ECAL active part characteristics.

3 ECAL equalization and calibration

The response of each anode is equalized using the signal deposited by proton and Helium MIPs selected with the help of the other AMS subdetectors: helium nuclei ionization is 4 times the one of protons and allows for a better energy resolution, on the other hand, protons are more frequent and allow to monitor temperature effects on a smaller time scale.

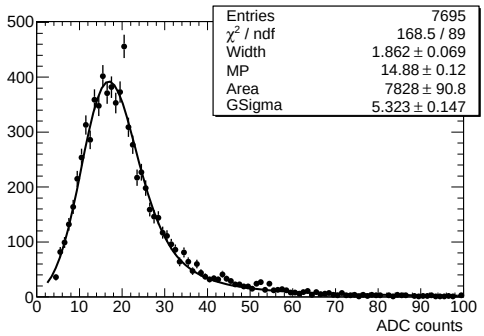

Figure 2: Typical distribution of MIP signal in an ECAL cell.

For each anode the equalization constant (in high gain ADC counts) is obtained from the value of the peak of the Landau distribution convoluted with a gaussian (fig.2) corresponding to the energy deposited by the MIPs hitting the central part of the anode.

The MIP energy deposit must be corrected for the effect of the light attenuation along the fiber. The attenuation factor A as function of the distance x from the PMT can be measured using MIPs or electrons impinging on the fiber at different distances from the PMT and is given by:

$$A(x) = fe^{(-x/\lambda_f)} + (1-f)e^{(-x/\lambda_s)}, \qquad (1)$$

where $\lambda_f = 110$ mm and $\lambda_s = 2605$ mm are the "fast" and "slow" attenuation constants respectively and $f = 0.17$ is the weight of the fast attenuation process.

Furthermore the MIP energy deposit must be corrected for temperature: using the temperature sensors located close to the PMT it's possible to correlate the anode energy response of each cell with its temperature (fig.3). The gain variation has been measured for each anode and is on average of $\sim$0.25% per degree.

The low gain channels equalization is obtained through the High/Low gain ratio obtained from the data in which both are present and far from saturation. The value of this ratio is very close to the design one (33) and stable in time at the per mille level [1].

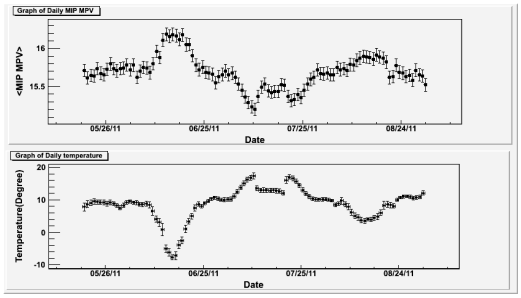

Figure 3: Correlation of MIP peak value with temperature.

Calibration of energy scale has been performed using the data from AMS test beam operated in Summer 2010 with the whole AMS detector in the final configuration.

Energy of electromagnetic particles is obtained in the following steps [2]:

- contiguous anodes are grouped to form first 1-dimensional clusters, then 2-dimensional clusters and finally the 3-dimensional shower;
- shower direction is estimated and light attenuation is applied;
- if the shower touches the lateral edges a lateral leakage correction is applied by using a mirror image of the energy deposited inside the calorimeter;
- a correction for the anode inefficiency close to the anode edges is applied using the ratio of the energy deposited in 1 Moliere radius with respect to the one deposited in 3 Moliere radius;
- a rear leakage correction is applied using the fraction of energy deposited in the last superlayer and the total energy deposited in the calorimeter.

By comparing the shower reconstructed energy with the electron and positron beam energy the energy scale factor to convert ADC counts to energy at T=23^{o}C has been obtained: 1 ADC count=0.470 MeV.

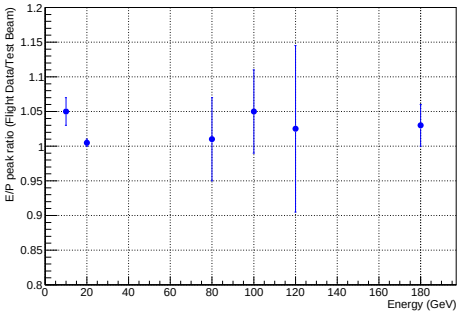

Figure 4: Ratio of Energy/Momentum ratio in flight and at 2010 Test Beam. Errors are dominated by beam statistics.

1. Low gain equalization has also been checked with a test beam [4] looking at the longitudinal shape of the energy deposited by electrons impinging on the detector at different position and angles.
2. A detailed description of the energy reconstruction procedure can be found in [2].

The stability of this energy scale has been checked on flight looking at the ratio between the electron energy, as measured by ECAL, and the electron momentum as measured by the Silicon Tracker: this ratio appears to be constant[3] before and after the launch once the temperature correction (from 23^{o}C to 10^{o}C) is applied (fig.4). Since the momentum scale is fixed by the permanent magnet also the energy scale must be constant.

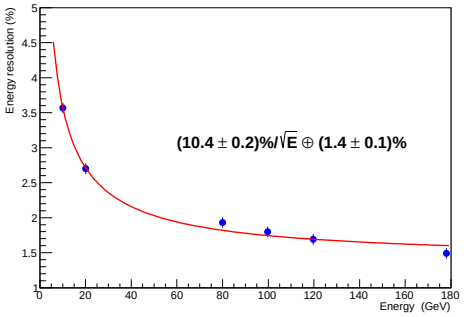

Figure 5: ECAL energy resolution measured at 2010 Summer test beam.

According to the results of the 2010 test beam ECAL energy resolution is (fig.5):

$$\sigma(E)/E = (10.4 \pm 0.2)\%/\sqrt{E(GeV)} \oplus (1.4 \pm 0.1)\% \quad (2)$$

and its linearity is better than 1% at least up to 300 GeV.

4 Angular resolution

The direction of the incoming particle is obtained from the shower by fitting the shower axis position in each layer of anodes. The axis position in each layer is usually defined as the center of energy of the shower in that layer. Nonetheless for electromagnetic particles with energy larger than 10 GeV a more precise determination of the axis position is obtained from the ratio between the energy deposited in the two cells close to the cell with the highest energy deposit in the layer: the logarithm of this "left-right ratio" is linearly correlated with the axis position obtained by extrapolating the track reconstructed by the Silicon Tracker.

The resulting angular resolution, $\Delta\theta_{68}$, defined as the angular width around the beam incidence angle that contains the 68% of the reconstructed angle is shown in fig. 6. The test beam result has been confirmed in flight by the study of the relative angle between the shower axis and the direction obtained from the Silicon Tracker, whose error is negligible with respect to the one of the shower axis [5].

5 Electron and positron identification

Discrimination between electromagnetic and hadronic showers is a key feature of ECAL.

In order to maximize the separation between protons and electrons or positrons, an electromagnetic classifier based on the Boosted Decision Tree (BDT) technique has been developed. The BDT technique uses a large set of experimental variables (the energy deposited and its transverse distribution in each ECAL layer, the total area and the number of cells with energy deposit associated to the shower) taking into account their correlation. By means of this technique all the calorimeter information can be exploited at maximum. The BDT is trained using both electron (signal) and proton (background) data samples selected by using the TRD information and the charge as measured by the Silicon Tracker. In order to reduce biases on the energy spectrum all the variables are normalized so to have the same distribution regardless of the electron energy.

ECAL energy is also used to reject protons requiring its matching with the incoming particle rigidity (R) measured by the tracker. By means of a cut on this ratio and of the BDT output value, preserving 90% efficiency for electrons and positrons, a proton rejection factor better than 10^3 can be obtained up to 1 TeV (fig. 7).

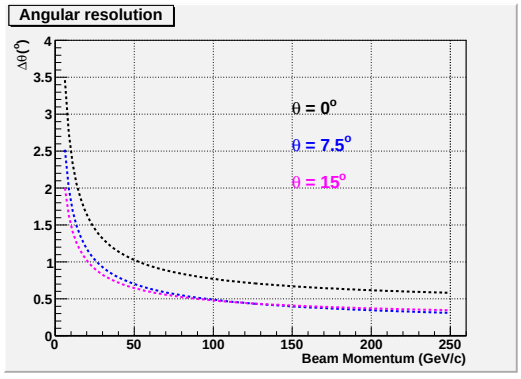

Figure 6: Angular resolution for different incidence angles.

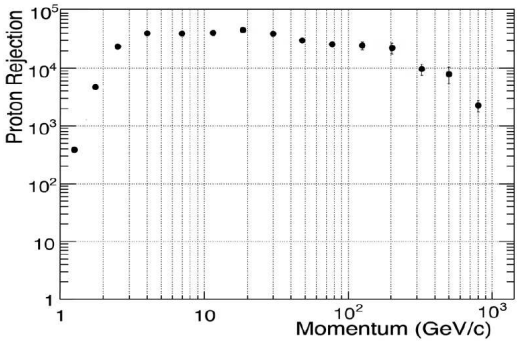

Figure 7: Proton rejection using ECAL BDT and an Energy/Rigidity cut (>0.75). Electron efficiency is 90%.

6 Photon identification

AMS-02 is able to detect photons in two complementary ways: the commonly used detection of conversions in electron/positron pairs and the identification of photons directly interacting on the calorimeter. With respect to the study of the photon conversions in e+e- pairs, direct photon detection has a larger statistics[4], excellent energy resolution and a similar angular resolution. In particular energy resolution is pivotal to reveal eventual structures in

3. The ratio is not 1 because of the electron bremsstrahlung.
4. Thanks to the reduced amount of material in front of ECAL.

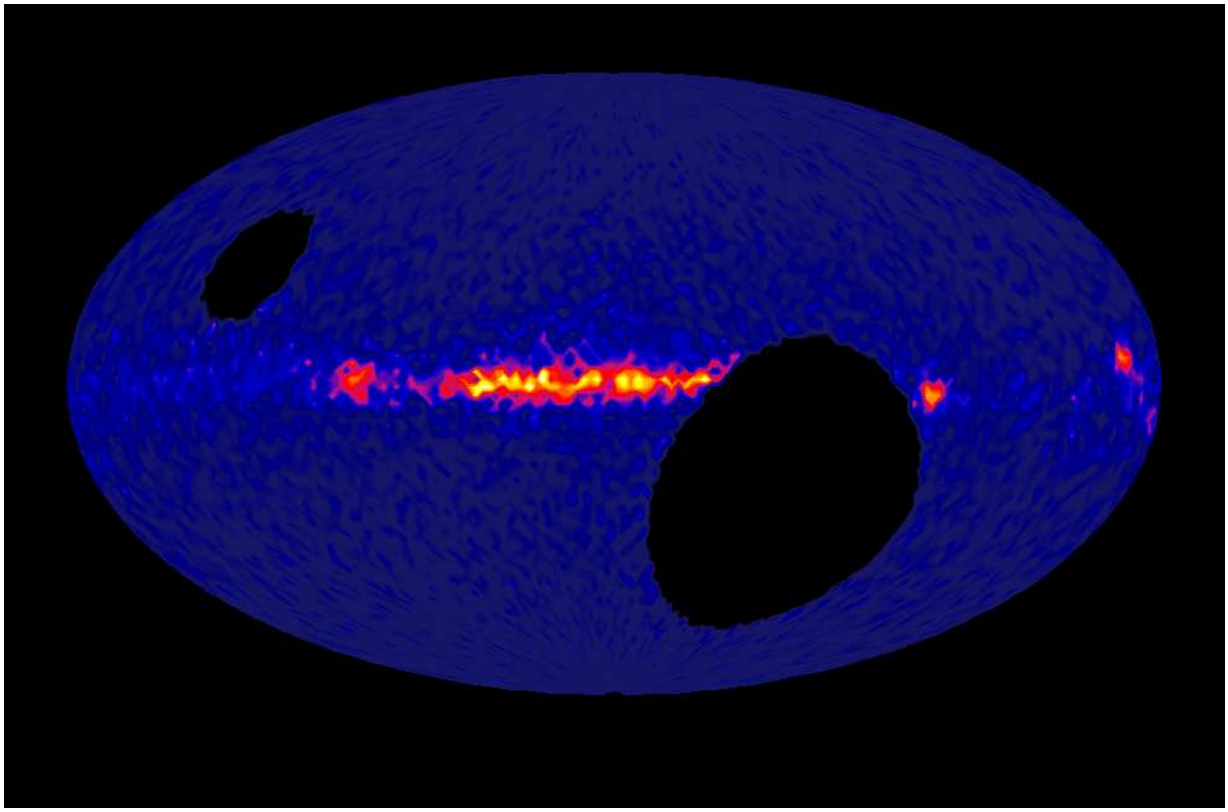

Figure 8: Gamma flux above 2 GeV in $2^o \times 2^o$ pixels in galactic coordinates observed by ECAL in 22 months.

the photon spectrum that would be a direct signature for dark matter annihilation.

A photon trigger, using only ECAL signals, is active during AMS-02 data taking and guarantees an efficiency higher than 90% above 2 GeV and higher than 99% above 5 GeV. The large amount of information available from sub-detectors ahead of ECAL largely reduces the probability for a charged particle to be identified as a photon. The main background is originated by protons and electrons reaching ECAL laterally and generating a shower whose axis is wrongly reconstructed. This background can be removed by means of a tight quality cut on the electromagnetic shower inside ECAL. The requirement of an electromagnetic shower strongly reduces the proton background. Charged particles crossing the AMS-02 detector are rejected asking for no reconstructed tracks in the silicon tracker or in TRD or in Time Of Flight (TOF) system. Furthermore, inside a cone surrounding the shower axis, single hits may be present only on 3 (or less) 3 tracker layers (excluding the one closest to ECAL) or in one upper TOF layer. The width of the cone around the shower axis is modulated with the ECAL energy to mimic the detectors behaviors for single track electrons. An irreducible background comes from electrons radiating hard bremsstrahlung photons on top of AMS detector but not releasing any track in TRD. This background is estimated with the help of the Monte Carlo of the detector. The low background level is confirmed by the sky map (fig. 8) obtained with photon candidates applying the correction for the detector exposure. In the map events are concentrated around the galactic plane and the brightest spots reveal the gamma emission from Vela, Geminga, Crab and Cygnus. The two empty ovals correspond to regions out of the AMS field of view used in this study. The energy threshold around 2 GeV is essentially due to the trigger. The possibility to identify known gamma sources confirms the high quality of the photon direction reconstructed only by the calorimeter.

7 Conclusions

AMS-02 calorimeter is performing very well in space. After two years of space operations, since May 2011, only 1 PMT out of 324 has stopped working. Equalization and calibration appear to be very stable once the small temperature effects are taken into account. The excellent energy resolution and imaging capability of ECAL has been used to identify electromagnetic particles and to measure their flux. More results are expected in the near future as soon as more statistics will be available, in particular concerning the electron flux up to 1 TeV and the investigation of structures in the photon spectrum.

Acknowledgment: This work is partly supported by Agenzia Spaziale Italiana under contract ASI-INFN I/002/13/0.

References

[1] M. Aguilar et al., Phys.Rev.Lett. 14, 141102 (2013) 1-10 doi:10.1103/PhysRevLett.110.141102
[2] C. Adloff et al., Nucl.Instr.Meth. A714 (2013) 147154 doi:10.1016/j.nima.2013.02.020
[3] F. Cadoux et al., IEEE Trans.Nucl.Sci. 55 (2008) 817-821 doi:10.1109/TNS.2008.918517
[4] S. Di Falco et al., Adv.Space Res. 45 (2010) 112-122 doi:10.1016/j.asr.2009.08.005
[5] M.Vecchi et al., this proceedings.